

Kyung-Hwan Na · Su-Il Pyun

Effects of SO_4^{2-} , $\text{S}_2\text{O}_3^{2-}$ and HSO_4^- ion additives on the pitting corrosion of pure aluminium in 1 M NaCl solution at 40–70 °C

Received: 18 October 2004 / Revised: 3 November 2004 / Accepted: 10 November 2004 / Published online: 10 June 2005
© Springer-Verlag 2005

Abstract Effects of sulphate (SO_4^{2-}), thiosulphate ($\text{S}_2\text{O}_3^{2-}$) and hydrogensulphate (HSO_4^-) ion additives on the pitting corrosion of pure aluminium in 1 M NaCl solution have been investigated at various solution temperatures T_s , 40–70 °C using potentiodynamic polarisation experiment, double current step experiment and scanning electron microscopy (SEM). From the analysis of the galvanostatic potential transients obtained from the double current step experiment, it was suggested that both SO_4^{2-} and $\text{S}_2\text{O}_3^{2-}$ ions retard the initiation of the etch pits, and that they also inhibit the passivation of the etch pits during the current interruption to promote the subsequent re-activation of the etch pits over the whole range of T_s . In contrast, it was found that HSO_4^- ions promote the initiation of the etch pits and at the same time, they enhance the passivation of the etch pits during the current interruption with rising T_s . From the SEM micrographs, it was revealed that as T_s increased the pit morphology changed from circular shape to irregular shape with rough surface in the presence of SO_4^{2-} or $\text{S}_2\text{O}_3^{2-}$ ions, but it changed to strip-like shape in the presence of HSO_4^- ions. The beneficial effects of anion additives on the increase in surface area were discussed on the basis of the morphological change of the etch pits in the presence of anion additives.

Keywords Aluminium · Pitting corrosion · Sulphate · Thiosulphate · Hydrogensulphate

Introduction

Capacitor has been one of major electronic components used in various electronic devices. Although such new capacitors as electric double-layer capacitor (EDLC) and multi-layer ceramic chip capacitors (MLCC) have been developed over the past few decades, the demand for aluminium (Al) electrolytic capacitors in electronic equipments has steadily increased because it has wide working potential range with favourable economics. Electrochemical etching of Al foil is an indispensable industrial process used for increasing surface area of Al foil. For high-voltage applications, DC etching which forms long etch tunnels is demanded rather than AC etching [1, 2].

In general, the etching process is done in a hot chloride solution at temperatures above 60 °C. In the initial attack, crystallographic cubic etch pits form. Since the pit walls grow in five directions simultaneously, the depth of etch pits is half the width at the surface [3]. When the etch pit width increases to about 1 µm, there is a change in pit growth morphology: the transformation of etch pits into etch tunnels and their subsequent growth along [100] direction occur [1]. On the other hand, below 60 °C, the formation of the macro-pits with nearly circular shape becomes dominant and their pit walls are composed of faceted surfaces [3].

In this respect, a considerable number of studies have been made on the Al dissolution kinetics in the etch pits [4], the passivation by the oxide film in the etch pits during the electrochemical etching process [5] and the morphological study of the etch pits by using scanning electron microscopy (SEM) [6, 7]. The morphology of the etch pits is affected by many factors. Among them, the well-discussed factors are (1) the properties of Al foil itself, such as impurities, grain size and cubicity, (2) the properties of the etching solution, such as composition, temperature and pH, and finally, (3) etching time.

Over the past few decades, various additives have been introduced to a hot chloride solution for increasing

K.-H. Na · S.-I. Pyun (✉)
Department of Materials Science and Engineering,
Korea Advanced Institute of Science and Technology,
373-1, Guseong-dong, Yuseong-gu, Daejeon,
305-701, Republic of Korea
E-mail: sipyun@webmail.kaist.ac.kr
Tel.: +82-42-8693319
Fax: +82-42-8693310

surface area of the Al electrode during the electrochemical etching process. Among them, sulphate (SO_4^{2-}) ion additives are the most common. In previous works from our laboratory [8, 9], the effects of SO_4^{2-} ion additives on the pitting corrosion of pure Al were investigated at room temperature by observing how the pit morphology depends on the concentration of SO_4^{2-} ion additives in the chloride solution. It was revealed that SO_4^{2-} ions retard pit initiation but at the same time, accelerate Al dissolution in the pits. However, little is known about their roles in the pitting corrosion of Al during the electrochemical etching process in a hot chloride solution. In addition, it was reported that thiosulphate ($\text{S}_2\text{O}_3^{2-}$) and hydrogensulphate (HSO_4^-) ion additives made a significant contribution to the increase of capacitance [10]. But there have been few studies on the mechanism for the enlargement of the surface area in the presence of $\text{S}_2\text{O}_3^{2-}$ or HSO_4^- ion additives.

Thus, the present work is aimed at investigating the effects of SO_4^{2-} , $\text{S}_2\text{O}_3^{2-}$ and HSO_4^- ion additives on the pitting corrosion of pure Al in 1 M sodium chloride (NaCl) solution at 40–70 °C using potentiodynamic polarisation experiment, double current step experiment, AC impedance spectroscopy and SEM. For this purpose, we first examined the roles of anion additives in the initiation and subsequent passivation of the etch pits. After that, the contribution of each process to the morphological change of the etch pits in the presence of anion additives was examined.

Materials and methods

In this work, the specimen was high purity (99.99%), 120- μm -thick Al foil. The chemical composition of the Al foil used in this study was determined by inductively coupled plasma atomic emission spectrometry, and the result is given in Table 1.

The Al foil specimen was previously immersed in 1 M NaOH solution at 25 °C for 10 min to enhance uniformity of the distribution of the etch pits [5, 11]. After doing so, the electrochemical experiments were performed in four kinds of solutions, i.e. 1 M NaCl, 1 M NaCl + 0.3 M Na_2SO_4 , 1 M NaCl + 0.3 M $\text{Na}_2\text{S}_2\text{O}_3$, 1 M NaCl + 0.3 M NaHSO_4 , at the solution temperatures T_s , 40, 55 and 70 °C. All the electrochemical measurements were made by employing a three-electrode electrochemical cell in which a platinum gauze and a silver–silver chloride electrode served as the counter and reference electrodes, respectively. The area of the foil specimen exposed to the solution amounted to 0.32 cm^2 .

The potentiodynamic polarisation experiment was carried out in the applied potential range from open-circuit potential to $-0.3 V_{\text{Ag}/\text{AgCl}}$ with a scan rate of 0.5 mV s^{-1} by using a Zahner IM6e electrochemical measurement unit. The pitting corrosion during the galvanostatic etching process was also studied by double current step experiment with the applied current wave-form, which is illustrated in Fig. 1. The double current step experiment involves the short current interruption between two current steps of I and II. For SEM observation, the foil specimen was galvanostatically etched by applying an anodic current density of 0.1 A cm^{-2} for 10 s in 1 M NaCl solution in the absence and presence of anion additives, and then the etched surface was thoroughly cleaned with distilled water and ethanol.

In order to determine the oxide film capacitance of the etched foil specimen, the etched foil specimen was anodised in 0.5 M H_3BO_3 + 0.05 M $\text{Na}_2\text{B}_4\text{O}_7$ solution at 25 °C. An anodic current density of $5 \times 10^{-4} \text{ A cm}^{-2}$ was applied until 30 V was reached, and then the foil specimen was held at 30 V for 30 min. AC impedance spectra were measured on the anodised foil specimen in 0.5 M H_3BO_3 + 0.05 M $\text{Na}_2\text{B}_4\text{O}_7$ solution at 25 °C with a Zahner IM6e impedance analyser, by applying an AC signal of 5 mV amplitude superimposed on open-circuit potential over the frequency range of 10^{-1} – 10^5 Hz.

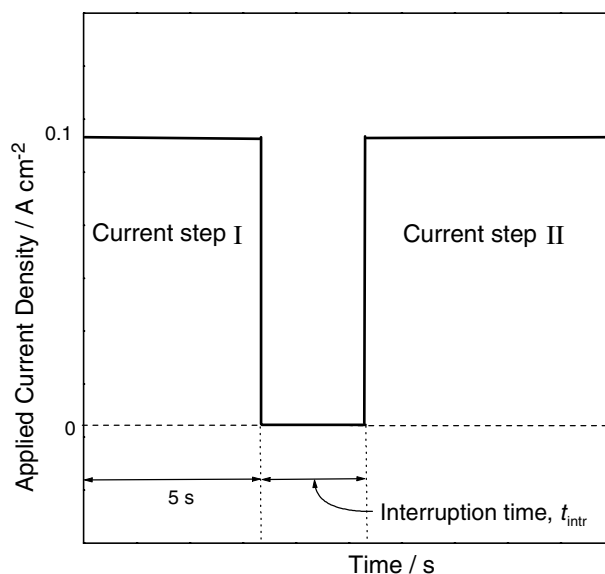


Fig. 1 Schematic diagram of applied current wave-form for the double current step experiment

Table 1 Impurity concentration in the pure Al foil specimen (in wt ppm)

Fe	Si	Cu	Mg	Zn	Mn	Cr	Ni	Ti	Pb	In
9.28	8.63	48.2	1.31	7.45	<1.0	<1.0	<2.0	<2.0	<5.0	<20

Results and discussion

Effects of anion additives on the initiation and passivation of the pits on the Al foil in NaCl solution

Figures 2a–c present the anodic polarisation curves at $T_s = 40, 55$ and 70 °C, respectively, measured on the foil specimen with a scan rate of 0.5 mV s^{-1} in 1 M NaCl solution in the absence and presence of SO_4^{2-} , $\text{S}_2\text{O}_3^{2-}$ and HSO_4^- ions. Firstly, the pitting potential E_{pit} in the presence of SO_4^{2-} ions was higher in value than E_{pit} in their absence, irrespective of the value of T_s , which implies that the Al foil becomes more resistant to the pitting corrosion in the NaCl solution containing SO_4^{2-} ions.

Secondly, the value of E_{pit} in the presence of $\text{S}_2\text{O}_3^{2-}$ ions was higher than that value in their absence at $T_s = 40$ and 55 °C, while E_{pit} showed almost the same value as E_{pit} in the absence at $T_s = 70$ °C, indicating that $\text{S}_2\text{O}_3^{2-}$ ions do not exert any noticeable effect on the pitting corrosion at $T_s = 70$ °C. Finally, the value of E_{pit} was decreased by the addition of HSO_4^- ions, regardless of the value of T_s , indicating the Al foil becomes more susceptible to the pitting corrosion in the presence of HSO_4^- ions.

One has usually discussed the susceptibility to the pitting corrosion in terms of E_{pit} determined from the anodic polarisation curves, as shown in Figs. 2a–c. However, such anodic polarisation curves provide little information on the pitting corrosion during the galvanostatic etching process which is generally used to increase the surface area of the Al foil. In this work, therefore, the double current step experiment was carried out to examine in detail the question of how various processes in the pitting corrosion (e.g. pit initiation, passivation and re-activation) are affected by the anion additives in NaCl solution during the galvanostatic etching process.

Figures 3a–c demonstrate the galvanostatic potential transients for current step I in the double current step experiment at $T_s = 40, 55$ and 70 °C, respectively, measured on the foil specimen in 1 M NaCl solution in the absence and presence of SO_4^{2-} , $\text{S}_2\text{O}_3^{2-}$ and HSO_4^- ions at an anodic current density of 0.1 A cm^{-2} before the current interruption. The potential transients represented by curves 2 and 4 in Fig. 3a, measured in the presence of SO_4^{2-} and HSO_4^- ions, respectively, at $T_s = 40$ °C, were truncated in shape due to the measuring limit of the equipment.

Apart from two transients, the other potential transients given in Figs. 3a–c clearly exhibited a three-stage behaviour. As the time progressed, the value of potential increased monotonically to a maximum value E_{max} at first, then decayed rapidly and finally remained constant. It is known [12, 13] that the first stage potential transient is associated with the double layer charging and the oxide film growth, and the second stage is attributed to

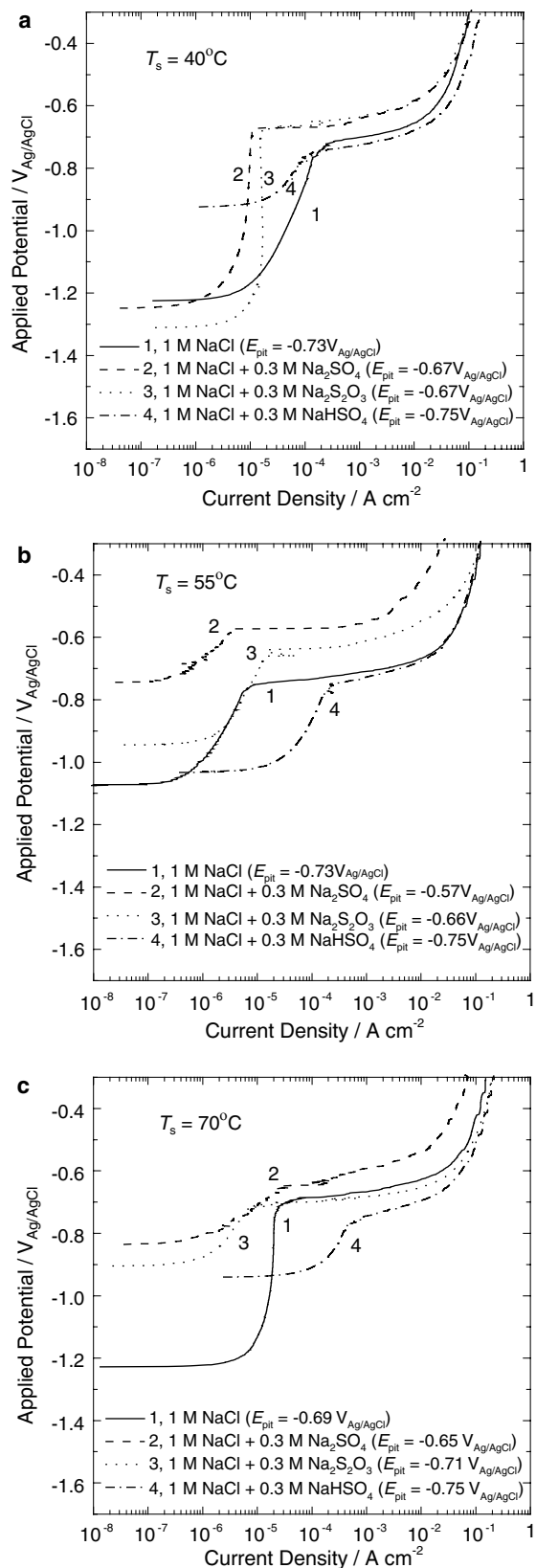


Fig. 2 Anodic polarisation curves measured on the Al foil specimen with a scan rate of 0.5 mV s^{-1} in 1 M NaCl solution in the absence and presence of SO_4^{2-} , $\text{S}_2\text{O}_3^{2-}$ and HSO_4^- ions at **a** 40 °C, **b** 55 °C and **c** 70 °C

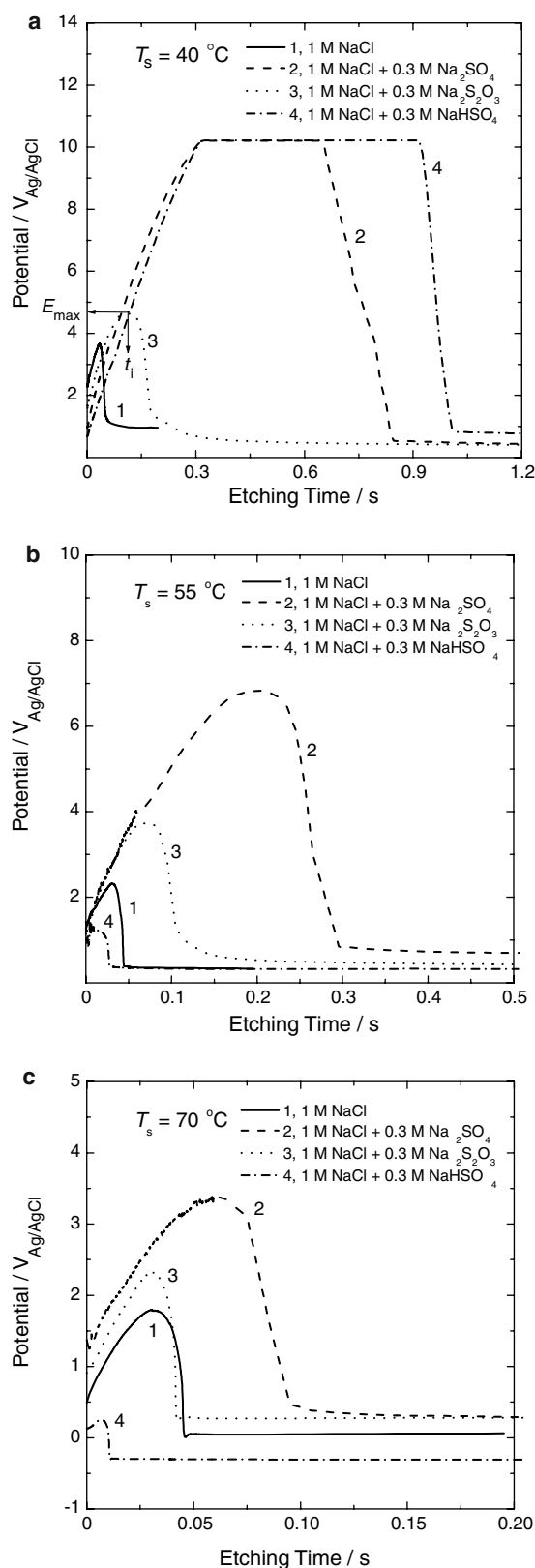
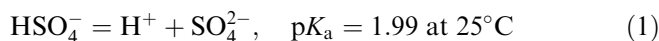


Fig. 3 Galvanostatic potential transients for current step I in the double current step experiment, measured on the Al foil specimen in 1 M NaCl solution in the absence and presence of SO_4^{2-} , $\text{S}_2\text{O}_3^{2-}$ and HSO_4^- ions at an anodic current density of 0.1 A cm^{-2} before the current interruption at **a** 40°C , **b** 55°C and **c** 70°C

the breakdown of the oxide film and to the etch pit initiation. Finally, the third stage represents the steady growth of etch pits. Here, the time to reach E_{max} was denoted as the induction time t_{in} which is necessary for the etch pit initiation.

It was found from Figs. 3a–c that E_{max} and t_{in} in the presence of SO_4^{2-} or $\text{S}_2\text{O}_3^{2-}$ ions were higher and longer than E_{max} and t_{in} in their absence, respectively, regardless of the value of T_s . This implies that etch pit initiation on the Al foil surface is greatly retarded by SO_4^{2-} or $\text{S}_2\text{O}_3^{2-}$ ions over the whole T_s range. Keeping in mind that the breakdown of the oxide film in NaCl solution is caused by the incorporation of Cl^- ions into the oxide film [8, 12, 14], it is reasonable to say that SO_4^{2-} or $\text{S}_2\text{O}_3^{2-}$ ions suppress the incorporation of Cl^- ions into the oxide film by the competitive adsorption with Cl^- ions, and hence they inhibit the etch pit initiation on the Al foil surface.

On the other hand, it is noticeable that the values of E_{max} and t_{in} were increased by the addition of HSO_4^- ions at $T_s = 40^\circ\text{C}$, but they were considerably decreased at $T_s = 55$ and 70°C , suggesting that HSO_4^- ions promote the etch pit initiation on the Al foil surface at high T_s above 55°C . In the presence of HSO_4^- ions, the pH value of NaCl solution is significantly lowered by the following dissociation reaction of HSO_4^- ions [15]:



where K_a is the dissociation constant and $\text{p}K_a = -\log K_a$. Accordingly, the enhancement of the etch pit initiation by HSO_4^- ions at high T_s above 55°C may result from the thermodynamic instability of the oxide film on the Al foil surface in a solution with low pH.

It is well known that pits stop growing when the surface of the pits is completely passivated, and hence the passivation behaviour is an important consideration in the phenomenon of etch pit growth during the galvanostatic etching process. In this respect, the galvanostatic potential transient obtained just after the short current interruption from the double current step experiment can offer important information about not only the passivation behaviour but also the subsequent re-activation behaviour during the galvanostatic etching.

Figures 4a–c demonstrate the galvanostatic potential transients for current step II in the double current step experiment at $T_s = 40, 55$ and 70°C , respectively, measured on the foil specimen in 1 M NaCl solution in the absence and presence of SO_4^{2-} , $\text{S}_2\text{O}_3^{2-}$ and HSO_4^- ions at an anodic current density of 0.1 A cm^{-2} just after the current interruption for $t_{\text{intr}} = 20 \text{ ms}$.

The measured potential transient in the absence of anion additives simply showed a monotonic potential decay with time at $T_s = 40^\circ\text{C}$, which means that etch pits are hardly passivated, but they are still active during the current interruption for $t_{\text{intr}} = 20 \text{ ms}$. From the fact that a potential overshoot emerged in the potential transient at high T_s above 55°C , however, it is readily inferred that most etch pits are completely passivated during the

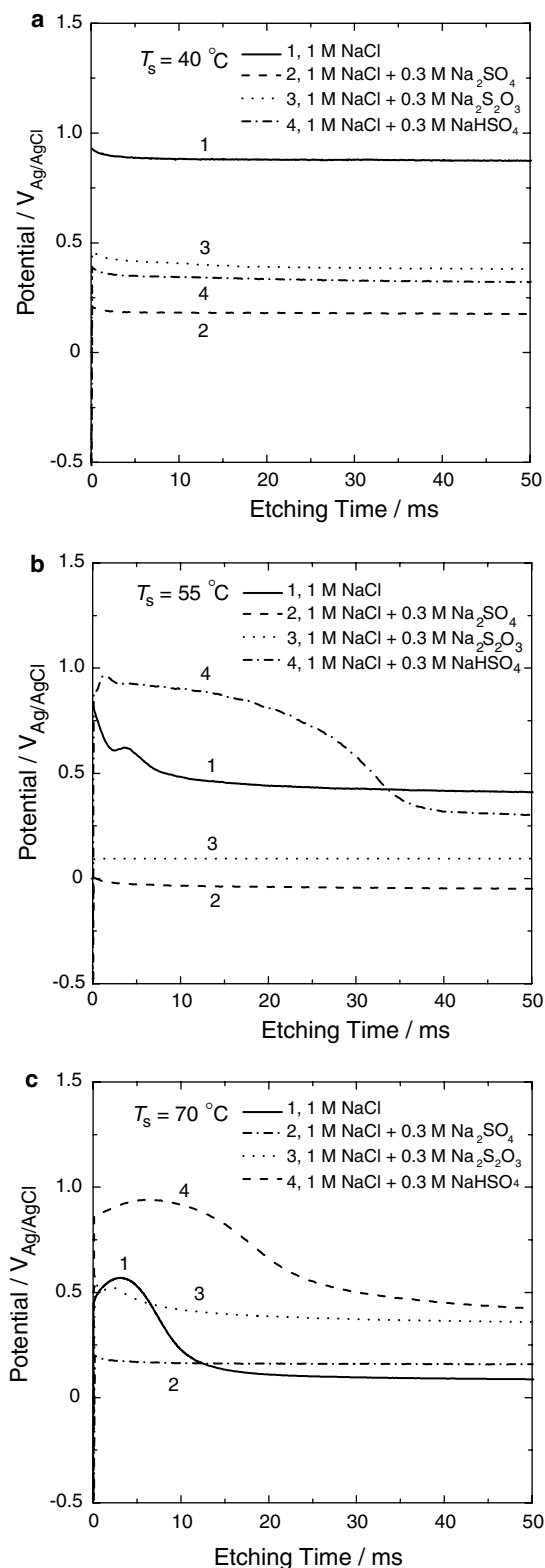


Fig. 4 Galvanostatic potential transients for current step II in the double current step experiment, measured on the Al foil specimen in 1 M NaCl solution in the absence and presence of SO_4^{2-} , $\text{S}_2\text{O}_3^{2-}$ and HSO_4^- ions at an anodic current density of 0.1 A cm^{-2} just after the current interruption for $t_{\text{intr}} = 20 \text{ ms}$ at **a** 40°C , **b** 55°C and **c** 70°C

current interruption and hence they are re-activated through the same consecutive steps as described in Fig. 3. This may be due to the fact [12, 16] that Cl^- ions retard the adsorption of OH^- ions, which participate in the dissolution reaction, resulting in reduced dissolution in the pit at high T_s .

On the other hand, it is worthwhile noting that the potential transient in the presence of SO_4^{2-} or $\text{S}_2\text{O}_3^{2-}$ ions exhibited a simple potential decay with time without showing any potential overshoot over the whole T_s range. From the analysis of potentiostatic current transients, Flis and Kowalczyk [12] suggested that the adsorbed Cl^- ions on the bare Al surface are partially replaced by SO_4^{2-} ions during the pitting corrosion. From the results, it is thus conceivable that a considerable number of the etch pits remain active in the NaCl solution containing SO_4^{2-} or $\text{S}_2\text{O}_3^{2-}$ ions, during the current interruption for $t_{\text{intr}} = 20 \text{ ms}$, even at $T_s = 55$ and 70°C , since SO_4^{2-} and $\text{S}_2\text{O}_3^{2-}$ ions partially replace Cl^- ions to enhance the dissolution of Al in the pit.

Similar to the case of SO_4^{2-} or $\text{S}_2\text{O}_3^{2-}$ ions, the potential transient in the presence of HSO_4^- ions at $T_s = 40^\circ\text{C}$ also showed a simple potential decay with time. However, an appreciable potential overshoot appeared at high T_s above 55°C . Moreover, it was observed that the potential overshoot in the presence of HSO_4^- ions was higher as compared with that in the absence. From the fact that the relatively more acidic conditions in the pit solution than the bulk solution, which are favourable to further pit growth, are hardly established in a solution with low pH, it is inferred that the etch pits tend to stop growing by passivation in the presence of HSO_4^- ions.

From the results of galvanostatic potential transients obtained from the double current step experiment, it is summarised that SO_4^{2-} and $\text{S}_2\text{O}_3^{2-}$ ions retard the initiation of the etch pits, and that they inhibit the passivation of the etch pits during the current interruption, which makes the subsequent re-activation of the etch pits during the pit growth easier over the whole T_s range. On the other hand, it was recognised that HSO_4^- ions promote the initiation of the etch pits, and at the same time they facilitate the passivation of the etch pits during the current interruption with rising T_s .

Effects of anion additives on the pit morphology of the Al foil in NaCl solution

Figure 5 illustrates the plots of the oxide film capacitance C_{ox} of the etched and anodised foil specimen against T_s . The AC impedance spectra were measured in $0.5 \text{ M H}_3\text{BO}_3 + 0.05 \text{ M Na}_2\text{B}_4\text{O}_7$ solution and analysed using the complex non-linear squares (CNLS) fitting method based upon the simple Randles circuit [17, 18].

The value of C_{ox} increased with rising T_s in all the solutions, and C_{ox} in the presence of SO_4^{2-} , $\text{S}_2\text{O}_3^{2-}$ or HSO_4^- ions was determined to be larger in value than C_{ox} in their absence at high T_s above 55°C . If we assume

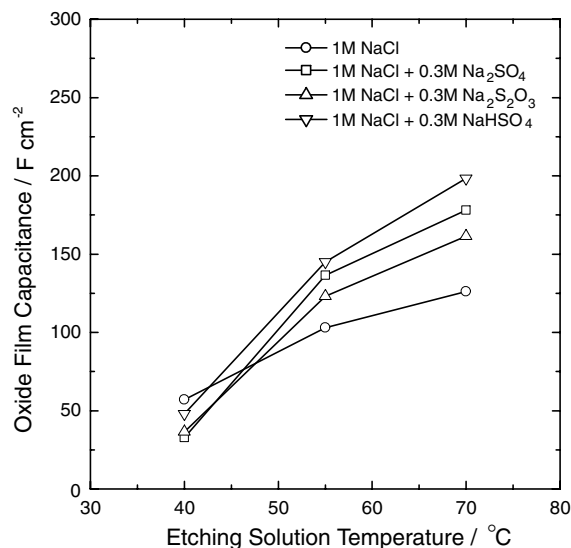


Fig. 5 Plots of the oxide film capacitance C_{ox} of the anodised Al foil specimen versus the etching solution temperature T_s determined from the AC impedance spectra measured in $0.5 \text{ M H}_3\text{BO}_3 + 0.05 \text{ M Na}_2\text{B}_4\text{O}_7$ solution at 25°C . The foil specimen was previously etched at a constant anodic current density of 0.1 A cm^{-2} for 10 s in 1 M NaCl solution in the absence and presence of SO_4^{2-} , $\text{S}_2\text{O}_3^{2-}$ and HSO_4^- ions. After that, the etched foil specimen was anodised in $0.5 \text{ M H}_3\text{BO}_3 + 0.05 \text{ M Na}_2\text{B}_4\text{O}_7$ solution at 25°C

that the values of the thickness and the dielectric constant of the oxide films are constant, the oxide film capacitance C_{ox} is proportional to the surface area. Therefore, it seems that the surface area of the etched foil specimen was increased by the addition of SO_4^{2-} , $\text{S}_2\text{O}_3^{2-}$ or HSO_4^- ions at high T_s above 55°C . In contrast, the value of C_{ox} in the presence of SO_4^{2-} , $\text{S}_2\text{O}_3^{2-}$ or HSO_4^- ions was lower than that value in their absence at $T_s = 40^\circ\text{C}$. This implies that the surface area of the etched foil specimen was decreased by the addition of SO_4^{2-} , $\text{S}_2\text{O}_3^{2-}$ or HSO_4^- ions at $T_s = 40^\circ\text{C}$.

Figures 6a–d depict the SEM micrographs of the foil specimen surface, galvanostatically etched at an anodic current density of 0.1 A cm^{-2} for 10 s in 1 M NaCl, 1 M NaCl + 0.3 M Na_2SO_4 , 1 M NaCl + 0.3 M $\text{Na}_2\text{S}_2\text{O}_3$, 1 M NaCl + 0.3 M NaHSO_4 solutions, respectively, at $T_s = 40^\circ\text{C}$. It is clear that macro-pits with nearly circular shape formed on the Al foil surface, regardless of the absence and presence of anion additives, and at the same time the crystallographic features of individual cubic etch pits were still visible at the orifices and walls of macro-pits. This strongly indicates that small cubic etch pits coalesced to form macro-pits during the galvanostatic etching process at $T_s = 40^\circ\text{C}$.

The SEM micrographs of the foil specimen surface galvanostatically etched in 1 M NaCl, 1 M NaCl + 0.3 M Na_2SO_4 , 1 M NaCl + 0.3 M $\text{Na}_2\text{S}_2\text{O}_3$, 1 M NaCl + 0.3 M NaHSO_4 solutions at $T_s = 70^\circ\text{C}$ were also given in Figs. 7a–d, respectively. Figure 7a showed that the small etch pits in the absence of anion additives were widely distributed over the foil surface at $T_s = 70^\circ\text{C}$.

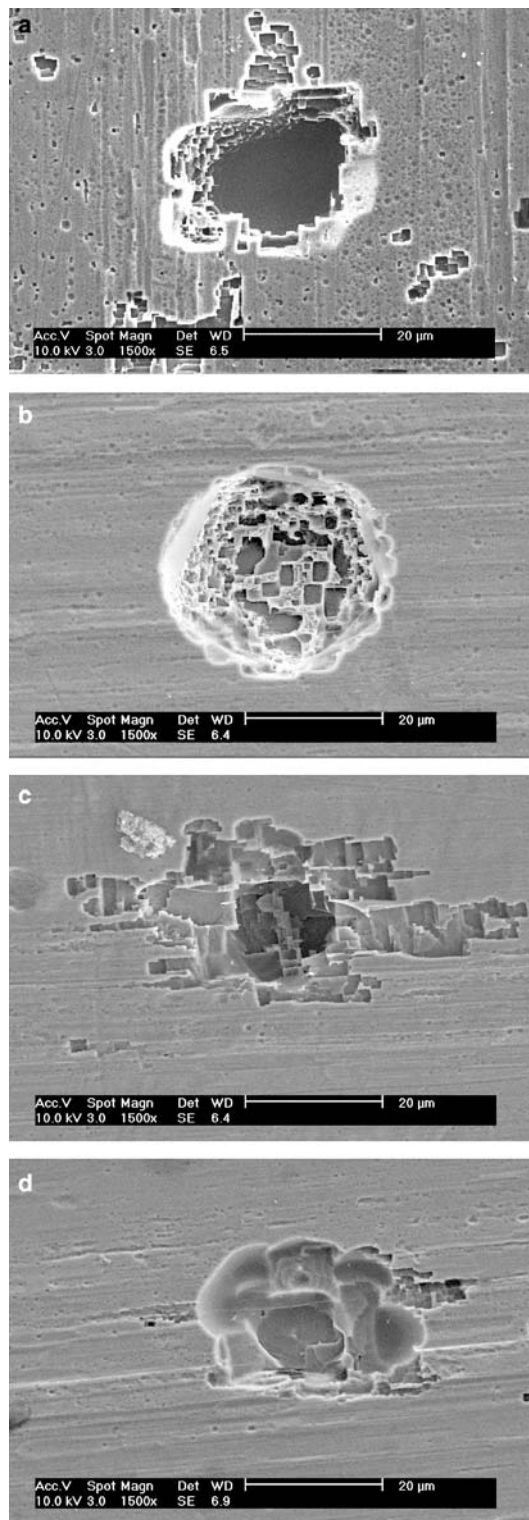


Fig. 6 SEM micrographs of the Al foil specimen surface galvanostatically etched at an anodic current density of 0.1 A cm^{-2} for 10 s in **a** 1 M NaCl, **b** 1 M NaCl + 0.3 M Na_2SO_4 , **c** 1 M NaCl + 0.3 M $\text{Na}_2\text{S}_2\text{O}_3$ and **d** 1 M NaCl + 0.3 M NaHSO_4 solutions at 40°C

In the presence of SO_4^{2-} or $\text{S}_2\text{O}_3^{2-}$ ions (Figs. 7b, c), the pit morphology changed from circular shape at $T_s = 40^\circ\text{C}$ to irregular shape with rough surface at

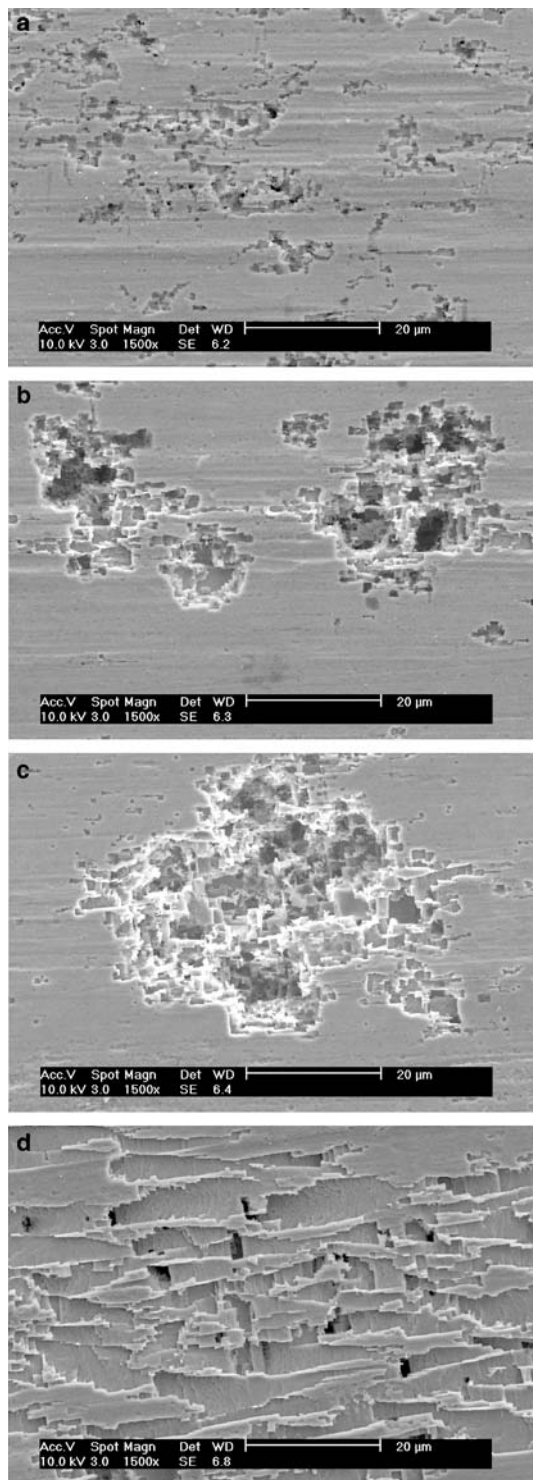


Fig. 7 SEM micrographs of the Al foil specimen surface galvanostatically etched at an anodic current density of 0.1 A cm^{-2} for 10 s in **a** 1 M NaCl, **b** 1 M NaCl + 0.3 M Na_2SO_4 , **c** 1 M NaCl + 0.3 M $\text{Na}_2\text{S}_2\text{O}_3$ and **d** 1 M NaCl + 0.3 M NaHSO_4 solutions at $70 \text{ }^\circ\text{C}$

$T_s = 70 \text{ }^\circ\text{C}$. In the previous work from our laboratory [8], it was reported that SO_4^{2-} ions in NaCl solution enhance the formation of the etch tunnels in the

macro-pits. Therefore, macro-pits, whose walls were roughened by the formation of the etch tunnels in the pits, may be responsible for the increase in the surface area of the etched foil specimen.

In the presence of HSO_4^- ions (Fig. 7d), it was observed that the pit morphology changed from circular shape at $T_s = 40 \text{ }^\circ\text{C}$ to strip-like shape at $T_s = 70 \text{ }^\circ\text{C}$. From the results of the galvanostatic potential transients in the double current step experiment, it is proposed that HSO_4^- ions enhance the etch pit initiation and simultaneously inhibit the etch pit growth in the downward direction at high T_s above $55 \text{ }^\circ\text{C}$; thereby, pits with strip-like shape are formed on the Al foil surface, resulting in the increase of the surface area.

Consequently, from the SEM micrographs it was revealed that macro-pits emerged in the presence of SO_4^{2-} or $\text{S}_2\text{O}_3^{2-}$ ions, whose walls were roughened by the formation of the etch tunnels. On the other hand, pits with strip-like shape appeared in the presence of HSO_4^- ions, originating from the promotion of the etch pit initiation on the specimen surface and the simultaneous suppression of the etch pit growth in the downward direction. These morphological changes in the presence of anion additives may lead to the increase of the surface area.

Acknowledgements The receipt of a research grant (grant No. R01-2000-000-00240-0) from Korea Science and Engineering Foundation is gratefully acknowledged. Incidentally, this work was partly supported by the Brain Korea 21 project. The authors are indebted to Dr. J.-W. Lee in the corrosion and interfacial electrochemistry research laboratory at KAIST for his helpful discussion.

References

1. Lin W, Tu GC, Lin CF, Peng YM (1997) *Corros Sci* 39:1531
2. Goad DGW, Uchi H (2000) *J Appl Electrochem* 30:285
3. Wiersma BJ, Hebert KR (1991) *J Electrochem Soc* 138:48
4. Tak Y, Sinha N, Hebert KR (2000) *J Electrochem Soc* 147:4103
5. Sinha N, Hebert KR (2000) *J Electrochem Soc* 147:4111
6. Dunn CG, Bolon RB, Alwan AS, Stirling AW (1971) *J Electrochem Soc* 118:381
7. Beck TR, Uchi H, Hebert KR (1989) *J Appl Electrochem* 19:69
8. Lee WJ, Pyun SI (2000) *Electrochim Acta* 45:1901
9. Pyun SI, Na KH, Lee WJ, Park JJ (2000) *Corrosion* 56:1015
10. Wernick S, Pinner R, Sheasby PG (1987) *The surface treatment and finishing of aluminium and its alloys*. ASM International, Metals Park. p190
11. Na KH, Pyun SI (2004) *J Solid State Electrochem* 8:935, DOI: 10.1007/s10008-004-0511-3
12. Flis J, Kowalczyk L (1995) *J Appl Electrochem* 25:501
13. Osawa N, Fukuoka K (2000) *Corros Sci* 42:585
14. Pyun SI, Moon SM (1999) *J Solid State Electrochem* 3:331
15. Dean JA (1999) *Lange's handbook of chemistry*. McGraw-Hill, New York. p8.20
16. Schwabe K, Voigt C (1969) *Electrochim Acta* 14:853
17. Macdonald JR (1972) *Impedance spectroscopy*. Wiley, New York. p180
18. Bae JS, Pyun SI (1994) *J Mater Sci Lett* 13:573